



LAWRENCE
LIVERMORE
NATIONAL
LABORATORY

Results from the Cuoricino (Zero-Neutrino Double Beta) Decay Experiment

C. Arnaboldi, D. R. Artusa, F. T. Avignone, M. Balata, I. Bandac, M. Barucci, J. W. Beeman, F. Bellini, C. Brofferio, C. Bucci, S. Capelli, L. Carbone, S. Cebrian, M. Clemenza, O. Cremonesi, R. J. Creswick, A. de Ward, S. Di Didomizio, M. J. Dolinski, H. A. Farach, E. Fiorini, G. Frossati, A. Giachero, A. Giuliani, P. Gorla, E. Guardincerri, T. D. Gutierrez, E. E. Haller, R. H. Maruyama, R. J. McDonald, S. Nisi, C. Nones, E. B. Norman, A. Nucciotti, E. Olivieri, M. Pallavicini, E. Palmieri, E. Pasca, M. Pavan, M. Pedretti, G. Pessina, S. Pirro, E. Previtali, L. Risegari, C. Rosenfeld, S. Sangiorgio, M. Sisti, A. R. Smith, L. Torres, G. Ventura, M. Vignati

October 22, 2008

Physical Review C

Disclaimer

This document was prepared as an account of work sponsored by an agency of the United States government. Neither the United States government nor Lawrence Livermore National Security, LLC, nor any of their employees makes any warranty, expressed or implied, or assumes any legal liability or responsibility for the accuracy, completeness, or usefulness of any information, apparatus, product, or process disclosed, or represents that its use would not infringe privately owned rights. Reference herein to any specific commercial product, process, or service by trade name, trademark, manufacturer, or otherwise does not necessarily constitute or imply its endorsement, recommendation, or favoring by the United States government or Lawrence Livermore National Security, LLC. The views and opinions of authors expressed herein do not necessarily state or reflect those of the United States government or Lawrence Livermore National Security, LLC, and shall not be used for advertising or product endorsement purposes.

Results from the CUORICINO $0\nu\beta\beta$ -decay experiment

(For submission to Physical Review C in November, 2007)

C. Arnaboldi¹, D.R. Artusa², F.T. Avignone III^{2#}, M. Balata³, I. Bandac², M. Barucci⁴,
J.W. Beeman⁵, F. Bellini¹⁴, C. Brofferio¹, C. Bucci³, S. Capelli¹, L. Carbone¹,
S. Cebrian⁶, M. Clemenza¹, O. Cremonesi¹, R.J. Creswick², A. de Ward⁷, S. Di
Didomizio⁸, M. J. Dolinski^{11,12}, H.A. Farach², E. Fiorini¹, G. Frossati⁷, A. Giachero³,
A. Giuliani⁹, P. Gorla^{1,6}, E. Guardincerri⁵, T. D. Gutierrez¹⁵, E.E. Haller^{5,10}, R.H.
Maruyama^{12,16}, R.J. McDonald⁵, S. Nisi³, C. Nones¹, E.B. Norman^{11,17}, A. Nucciotti¹,
E. Olivieri⁴, M. Pallavicini⁸, E. Palmieri¹³, E. Pasca⁴, M. Pavan¹, M. Pedretti⁹, G.
Pessina¹, S. Pirro¹, E. Previtali¹, L. Risegari⁴, C. Rosenfeld², S. Sangiorgio⁹, M. Sisti¹,
A.R. Smith⁵, L. Torres¹, G. Ventura⁴, M. Vignati¹⁴.

¹ Dipartimento di Fisica dell'Università di Milano-Bicocca e Sezione di Milano dell'INFN Milan
I-20126, Italy

² Department of Physics and Astronomy, University of South Carolina, Columbia, South Carolina
29208, USA

³ INFN Laboratori Nazionali del Gran Sasso, I-67010, Assergi (L'Aquila), Italy

⁴ Dipartimento di Fisica dell'Università di Firenze e Sezione di Firenze dell'INFN,
Firenze I- 50125, Italy

⁵ Lawrence Berkeley National Laboratory, Berkeley, California 94720, USA,

⁶ Laboratorio de Fisica Nuclear y Altas Energias, Universidad de Zaragoza, 50001 Zaragoza, Spain

⁷ Kamerling Onnes Laboratory, Leiden University, 2300 RAQ, Leiden

⁸ Dipartimento di Fisica dell'Università di Genova e Sezione di Genova dell'INFN, Genova I-16146, Italy

⁹ Dipartimento di Fisica e Matematica dell'Università dell'Insubria e Sezione di Milano dell'INFN, Como
I-22100, Italy

¹⁰ Department of Materials Science and Engineering, University of California, Berkeley, California
94720, USA

¹¹ Lawrence Livermore National Laboratory, Livermore, California 94551, USA

¹² Department of Physics, University of California, Berkeley, CA 94720, USA

¹³ INFN Laboratori Nazionali di Legnaro, Via Romea 4, I-35020 Legnaro, (Padova), Italy

¹⁴ Dipartimento di Fisica dell'Università di Roma La Sapienza e Sezione di Roma dell'INFN, Roma
I-00185, Italy

¹⁵ Physics Department, California Polytechnic State University, San Luis Obispo, CA 93407 USA

¹⁶ Department of Physics, University of Wisconsin, Madison, WI 53706 USA

¹⁷ Department of Nuclear Engineering, University of California, Berkeley, CA 94720, US

Recent results from the CUORICINO ^{130}Te zero-neutrino double-beta ($0\nu\beta\beta$) decay experiment are reported. CUORICINO is an array of 62 tellurium oxide (TeO_2) bolometers with an active mass of 40.7 kg. It is cooled to ~ 8 mK by a dilution refrigerator shielded from environmental radioactivity and energetic neutrons. It is running in the Laboratori Nazionali del Gran Sasso (LNGS) in Assergi, Italy. These data represent 11.83 kg y or 90.77 mole-years of ^{130}Te . No evidence for $0\nu\beta\beta$ -decay was observed and a limit of $T_{1/2}^{0\nu}(^{130}\text{Te}) \geq 3.0 \times 10^{24}$ y (90% C.L.) is set. This corresponds to upper limits on the effective mass, $\langle m_\nu \rangle$, between 0.19 and 0.68 eV when analyzed with the many published nuclear structure calculations. In the context of these nuclear models, the values fall within the range corresponding to the claim of evidence of $0\nu\beta\beta$ -decay by H.V. Klapdor-Kleingrothaus and his co-workers. The experiment continues to acquire data.

Corresponding author

This work performed in part under the auspices of the U.S. Department of Energy by Lawrence Livermore National Laboratory under Contract DE-AC52-07NA27344.

I. INTRODUCTION

There are three very important open questions in neutrino physics that can best be addressed by next generation zero-neutrino double-beta decay experiments. First, are neutrinos Majorana particles that differ from antineutrinos only by helicity? Second, what is their mass-scale? Third, is lepton number conservation violated? While searches for $\beta\beta$ -decay have been carried out steadily throughout many decades [1-3], it is now an interesting time for the field. The recent discoveries of and measurements of atmospheric and solar neutrino oscillations have shown that there exist scenarios in which the effective Majorana mass of the electron neutrino could be larger than 0.05 eV. Recent developments in detector technology make the observation of $0\nu\beta\beta$ -decay at this scale now feasible. For recent comprehensive experimental and theoretical reviews see [4-6]. Optimism that a direct observation of $0\nu\beta\beta$ -decay is possible was greatly enhanced by the observation and measurement of the oscillations of atmospheric neutrinos [7], the confirmation of oscillations of the chemical solar neutrino experiments [8-10] by SuperKamiokande [11], and the results of the SNO experiment [12] that clearly showed that the total flux of ^8B neutrinos from the sun predicted by Bahcall and his co-workers [13] is correct. Finally, the KamLAND reactor-neutrino experiment gave clear evidence that the MSW large mixing-angle solution of solar neutrino oscillations is the strongly favored one [14]. This important list of results published since 1998 weighs very heavily in favor of supporting two or more next generation $0\nu\beta\beta$ -decay experiments (see the reports in references [15,16]).

The most sensitive limits have come from germanium detectors enriched in ^{76}Ge . They were the Heidelberg-Moscow experiment ($T_{1/2}^{0\nu}(^{76}\text{Ge}) \geq 1.9 \times 10^{25} \text{ y}$) [17] and the IGEX experiment ($T_{1/2}^{0\nu}(^{76}\text{Ge}) \geq 1.6 \times 10^{25} \text{ y}$) [18]. These bounds imply that the effective Majorana mass of the electron neutrino, $\langle m_\nu \rangle$, defined below, ranges from 0.29 to 1.0-eV, depending on the choice of nuclear matrix elements used in the analysis. However, recently, a subset of the Heidelberg-Moscow Collaboration has reanalyzed the data and claimed evidence of a peak at the total decay energy, 2039-keV, implying $0\nu\beta\beta$ -decay [19,20]. While this has not been widely accepted by the neutrino community [21-23], there is no clear proof that the observed peak is not an indication of $0\nu\beta\beta$ -decay. The GERDA experiment, a ^{76}Ge experiment, being constructed in the Laboratori Nazionali del Gran Sasso (LNGS), will test this claim [24]. The CUORICINO experiment, also located at LNGS, is currently the most sensitive high-energy-resolution $0\nu\beta\beta$ -decay experiment in operation [25,26]. It is searching for the $0\nu\beta\beta$ -decay of ^{130}Te and has the capability of confirming the claim; however, a null result cannot be used to refute the claim because of the uncertainty in the nuclear matrix element calculations. The proposed Majorana ^{76}Ge experiment [27], CUORE ^{130}Te experiment [28], and ^{136}Xe EXO experiment [29] are all designed to reach the $\langle m_\nu \rangle \approx 0.05$ -eV mass sensitivity and below. Descriptions of other proposed experiments are given in the recent reviews [4-6].

There are other constraints on the neutrino-mass scale, irrespective of their Majorana or Dirac character. The Troitsk [30] and Mainz [31] ^3H single β -decay experiments have placed an upper limit of 2.2 eV on the mass of the electron neutrino.

The KATRIN experiment, a greatly enlarged ^3H β -decay experiment in preparation, is projected to have a sensitivity of 0.2-eV [32].

Recent astrophysical data are also very relevant in a discussion of neutrino mass. In a recent paper by Barger et al., [33] an upper limit on the sum of neutrino mass eigenvalues, $\Sigma = m_1 + m_2 + m_3 \leq 0.75\text{eV}$ (95% C.L.), was derived. The data used were from the Sloan Digital Sky Survey (SDSS) [34], the two degree Field Galaxy Red Shift Survey (2dFGRS) [35], and the Wilkinson Microwave Anisotropy Probe (WMAP) [36], as well as other CMB experiments and data from the Hubble Space Telescope. Hannestad [37] used the WMAP and 2dFGRS data to derive the bound $\Sigma < 1.0\text{-eV}$ (95%C.L.) and concluded that these data alone could not rule out the evidence claimed in [19,20]. On the other hand, Allen, Schmidt and Briddle [38] found a preference for a non-zero neutrino-mass i.e., $\Sigma = 0.56^{+0.30}_{-0.25}\text{eV}$. This is interestingly close to the favored range of values given in [19,20]. For recent papers on the subject see [39] and references therein. The constraint $\Sigma \leq 0.75\text{eV}$ would imply that the lightest neutrino eigenstate mass $\leq 0.24\text{eV}$. On the other hand, if the claim of the positive value Σ is correct, $m_1 \approx 0.17\text{eV}$, and next generation $0\nu\beta\beta$ -decay experiments would constitute a stringent test of lepton-number conservation, irrespective of the neutrino mass hierarchy. (see discussion of hierarchy below).

In this paper we present a detailed description and present the results from the CUORICINO $0\nu\beta\beta$ -decay experiment derived from data taken between April 2003 and May 2006. Finally, we note that ^{130}Te has a series of calculated matrix elements implying values of $\langle m_\nu \rangle$, derived from the CUORICINO half-life limit, as small as 0.2-eV, and as large as $\sim 0.68\text{-eV}$. A detailed discussion of very recent developments in the theoretical nuclear structure calculations is given later.

II. NEUTRINO PHYSICS AND NEUTRINOLESS DOUBLE-BETA DECAY

Neutrino oscillation data very strongly imply that there are three eigenstates that mix and have mass. The flavor eigenstates, $|\nu_{e\mu\tau}\rangle$, are connected to the mass eigenstates, $|\nu_{123}\rangle$, via a linear transformation:

$$|\nu_\ell\rangle = \sum_{j=1}^3 |U_{\ell j}^L| e^{i\delta_j} |\nu_j\rangle, \quad (1)$$

where $\ell = e, \mu, \tau$, and the factor $e^{i\delta_j}$ is a CP phase, ± 1 for CP conservation.

The decay rate for the $0\nu\beta\beta$ -decay mode driven by the exchange of a massive Majorana neutrino is expressed in the following approximation:

$$(T_{1/2}^{0\nu})^{-1} = G^{0\nu}(E_0, Z) \left| \frac{\langle m_\nu \rangle}{m_e} \right|^2 \left| M_f^{0\nu} - (g_A/g_V)^2 M_{GT}^{0\nu} \right|^2, \quad (2)$$

where $G^{0\nu}$ is a phase space factor including the couplings, $|\langle m_\nu \rangle|$ is the effective Majorana mass of the electron neutrino discussed below, $M_f^{0\nu}$ and $M_{GT}^{0\nu}$ are the Fermi and Gamow-Teller nuclear matrix elements respectively, and g_A and g_V are the relative axial vector and vector weak coupling constants respectively. After multiplication by a diagonal matrix of Majorana phases, $\langle m_\nu \rangle$ is expressed in terms of the first row of the 3×3 matrix of equation (1) as follows:

$$|\langle m_\nu \rangle| \equiv \left| \left(u_{e1}^L \right)^2 m_1 + \left(u_{e2}^L \right)^2 m_2 e^{i\phi_2} + \left(u_{e3}^L \right)^2 m_3 e^{i(\phi_3 + \delta)} \right|, \quad (3)$$

where $e^{i\phi_{2,3}}$ are the Majorana CP phases (± 1 for CP conservation in the lepton sector). Only the phase angle δ appears in oscillation experiments. The two Majorana phases, $e^{i\phi_{2,3}}$, do not appear in neutrino oscillation expressions and hence have no effect on them. The oscillation experiments have, however, constrained the mixing angles and thereby the u_{ij}^L coefficients in equation (3). Using the best-fit values from the SNO and Super Kamiokande solar neutrino experiments and the CHOOZ [40], Palo Verde [41] and KamLAND [14] reactor neutrino experiments, we arrive at the following expression in the case of the normal hierarchy:

$$|\langle m_\nu \rangle| \equiv \left| (0.70_{-0.04}^{+0.02}) m_1 + (0.30_{-0.02}^{+0.04}) m_2 e^{i\phi_2} + (\leq 0.05) m_3 e^{i(\phi_3 + \delta)} \right|, \quad (4)$$

where the errors were approximated from the published confidence level values. The bound on $|u_{e3}^L|^2$ is at a 95% CL and the errors on the first two coefficients are 1σ . In this convention, the expression for this expression in the case of the inverted hierarchy is obtained by exchanging $m_1 \Leftrightarrow m_3$.

The results of the solar neutrino and atmospheric neutrino experiments yield the mass square differences $\delta_{ij}^2 = |m_i^2 - m_j^2|$ but cannot distinguish between two mass patterns (hierarchies): the “normal” hierarchy, in which $\delta m_{solar}^2 = m_2^2 - m_1^2$ and $m_1 \cong m_2 \ll m_3$, and the “inverted” hierarchy where $\delta m_{solar}^2 = m_3^2 - m_2^2$ and $m_3 \cong m_2 \gg m_1$. In both cases we can approximate, $\delta m_{AT}^2 \cong m_3^2 - m_1^2$. Considering the values in equation (4), we make the simplifying approximation $(u_{e3}^L)^2 \ll (u_{e1,e2}^L)^2$ and we set $(u_{e3}^L)^2 \approx 0$. Using the central values of equation (4), we can write the following approximate expressions:

$$|\langle m_\nu \rangle| \cong m_1 \left| 0.7 + 0.3 e^{i\phi_2} \sqrt{1 + \frac{\delta_{solar}^2}{m_1^2}} \right|, \quad (5)$$

for the case of “normal” hierarchy, and,

$$|\langle m_\nu \rangle| \cong \sqrt{m_1^2 + \delta m_{AT}^2} \left| 0.7 + 0.3 e^{i\phi_3} \right|, \quad (6)$$

in the “inverted” hierarchy case. There is of course no experimental evidence favoring either hierarchy. In Table 1, we use equations (5) and (6) to show the predicted central

values of $\langle m_\nu \rangle$ as a function of the lightest neutrino mass eigenvalue, m_1 . These values define the desired target sensitivities of next generation $0\nu\beta\beta$ -decay experiments.

It is clear that a next generation experiment should have at least the sensitivity for discovery in the case of an inverted hierarchy when $e^{i\phi_2} = e^{i\phi_3}$ and for $m_1=0$. In this case, $\langle m_\nu \rangle \approx \sqrt{\delta_{AT}^2} \approx 0.050 \text{ eV}$. It should also be capable of being expanded in case this level is reached and no effect is found [15,16].

It is convenient to define the nuclear structure factor, F_N , (sometimes denoted as C_{mm} in the literature) as follows:

$$F_N \equiv G^{0\nu} \left| M_f^{0\nu} - (g_A / g_V)^2 M_{GT}^{0\nu} \right|^2 \quad (7)$$

Accordingly, the effective Majorana mass of the electron neutrino is connected to the half-life as follows:

$$\langle m_\nu \rangle = \frac{m_e}{\sqrt{F_N T_{1/2}^{0\nu}}} . \quad (8)$$

Possible interpretations of the null result of CUORICINO, in terms of the effective Majorana neutrino mass, may be understood with detailed analyses of the nuclear matrix elements discussed in a later section. Later, this null result will be compared with the positive claim reported in [19,20].

III. THE EXPERIMENT

The CUORICINO experiment is an array of cryogenic bolometers containing the parent isotope. This technique was suggested for $\beta\beta$ -decay searches by Fiorini and Niinikoski [42] and applied earlier by the Milano group in the MIBETA experiment [43]. The bolometers are sensitive calorimeters that measure the energy deposited by particle or photon interactions by measuring the corresponding rise in temperature. The CUORICINO bolometers are single crystals of TeO_2 ; they are dielectric and diamagnetic, and are operated at temperatures between 8 and 10 mK [44,45]. According to the Debye Law, the specific heat of TeO_2 crystals is given by $C(T) = \beta(T/\Theta_D)^3$, where $\beta = 1994 \text{ JK}^{-1} \text{ mol}^{-1}$ and Θ_D is the Debye temperature. In these materials, $C(T)$ is due almost exclusively to lattice degrees of freedom. In this case, Θ_D was specially measured for $5 \times 5 \times 5 \text{ cm}^3$ TeO_2 crystals as 232 K [43], which differs from the previously published value of 272K [46]. The specific heat followed the Debye Law down to 60 mK. The heat capacity of these crystals, extrapolated to 10 mK, is $2.3 \times 10^{-9} \text{ JK}^{-1}$. With these values of the parameters, an energy deposition of a few keV will result in a measurable temperature increase, ΔT . In CUORICINO, ΔT is measured by high-resistance germanium thermistors glued to each crystal. More details can be found in reference [44] and in earlier publications [47-49]. Accordingly, the temperature increase caused by the deposition of energy equal to the total $\beta\beta$ -decay energy, $|Q_{\beta\beta}| = 2530.3 \pm 2.0 \text{ keV}$, would

be $1.77 \times 10^{-4} K$. To obtain usable signals for such small temperature changes, very sensitive thermistors are required.

The thermistors are heavily doped high-resistance germanium semiconductors with an impurity concentration slightly below the metal-insulator transition. High quality thermistors require a very homogeneous doping concentration. For the CUORICINO Neutron Transmutation Doped (NTD) thermistors, this was achieved by means of a uniform thermal neutron irradiation throughout the entire volume, when they were irradiated in a nuclear reactor. The electrical conductivity of these devices depends very sensitively on the temperature because of variable range hopping (VRH) mechanisms. The resistivity varies with temperature according to $\rho = \rho_0 \exp(T_0/T)^\gamma$, where ρ_0, T_0 and γ all depend on the doping concentration. In the case of thermistors operating with VRH mechanisms, $\gamma = 1/2$.

Thermistors can be parameterized by their sensitivity, $A(T)$, defined as follows: $A(T) = |d(\ln R)/d(\ln T)| = \gamma(T_0/T)^\gamma$, and where the resistance is $R(T) = R_0 \exp(T_0/T)^\gamma$. The parameter $R_0 = \rho_0(d/a)$, where d and a are the distance between the contacts and the cross section of the thermistor, respectively. The values of R_0, T_0 and γ must be experimentally measured for each thermistor. This is done by coupling the thermistor to a low-temperature heat sink with a high heat-conductivity epoxy. The base temperature of the heat sink is between 15 and 50 mK. A current flows through the device and a V-I load curve is plotted. The curve becomes very non-linear due to the power dissipation, which causes the dynamic resistance, the slope of the I(V) curve, to invert from positive to negative. Indeed, the characterization, as discussed in reference [50] is done on the thermistors directly mounted on a heat sink, while the optimum bias is studied for the complete detector, thermistor and crystal, since the noise figure depends on all thermal conductances, glue, wires, Teflon etc. This maximizes the signal to noise ratio. The parameters of each thermistor are determined from a combined fit to a set of load curves determined at different base temperatures. A detailed description of the characterization process for Si thermistors was described in reference [50] and same process was used for the CUORICINO Ge thermistors.

The thermistors used in the MIBETA and CUORICINO experiments were produced at the Lawrence Berkeley National Laboratory and the University of California, Berkeley [51]. It is necessary to optimize the neutron doping of the Ge. This is facilitated by foils of metal with long-lived (n, γ) radioactive daughter nuclides, which allow the neutron exposure to be evaluated without having to wait for the intense radiation of the ^{71}Ge in the Ge sample to decay. Following the decay period, the Ge is heat treated to repair the crystal structure and then cut into 3x3x1 mm strips. Electrical connections are made with two 50 μm gold wires, ball bonded to metalized surfaces on the thermistor. The thermistors are glued to each bolometer by 9 spots of epoxy, deposited by an array of pins for better control of the thermal conductances and to minimize stresses at the interface between the two materials.

IV. THE CUORICINO DETECTOR

The Cryogenic Underground Observatory for Rare Events (CUORE) is a proposed array of 988 TeO_2 bolometers of about 750 g each, arranged in 19 towers, each similar to the CUORICINO, with one exception. The planes number 11 and 12 in the CUORICINO tower presently operating in the LNGS, contain smaller crystals; this is unique to CUORICINO. More details on CUORICINO and CUORE can be found in references [25,26,43,44].

As shown in Figure 1, the CUORICINO structure is as follows: each of the upper 10 planes and the lowest one consists of four $5 \times 5 \times 5 \text{ cm}^3$ TeO_2 crystals of natural isotopic abundance of ^{130}Te , as shown in the upper right hand figure, while the 11th and 12th planes have nine, $3 \times 3 \times 6 \text{ cm}^3$ crystals, as shown in the lower right hand figure. In the $3 \times 3 \times 6 \text{ cm}^3$ planes the central crystal is fully surrounded by the nearest neighbors.

The smaller crystals are of natural isotopic abundance except for four. Two of them are enriched to 82.3% in ^{128}Te and two are enriched to 75% in ^{130}Te . All crystals were grown with pre-tested low radioactivity material by the Shanghai Institute of Ceramics and shipped to Italy by sea to minimize the activation by cosmic ray interactions. They were lapped with specially selected low contamination polishing compound. All these operations, as well as the mounting of the tower, were carried out in a nitrogen atmosphere glove box in a clean room. The mechanical structure is made of oxygen-free high-conductivity copper and Teflon, and both were previously tested to be sure that measurable radioactive contaminations were minimal and consistent with the required detector sensitivity.

Thermal pulses are recorded by means of the NTD Ge thermistors thermally coupled to each crystal. The thermistors are biased through two high-impedance load resistors at room temperature, with resistances typically in excess of one hundred times that of the thermistors. The large ratio of the resistances of the load resistors over those of the thermistors allows the parallel noise to be kept at an adequate level. Low frequency noise from the load resistors was also minimized by design [52]. The voltage signals resulting from a particle interaction in the crystal are amplified and filtered before being fed to an analog-to-digital converter (ADC). This part of the electronic system is DC coupled, and only low-pass anti-aliasing filters are used to reduce the high-frequency noise. The typical bandwidth is approximately 10 Hz, with signal rise and decay times of order 30 and 500 ms, respectively. This entire electronic chain makes a negligible contribution to the detector energy resolution. More details of the design and features of the electronic system are found in [53]. The gain of each bolometer is calibrated and stabilized by

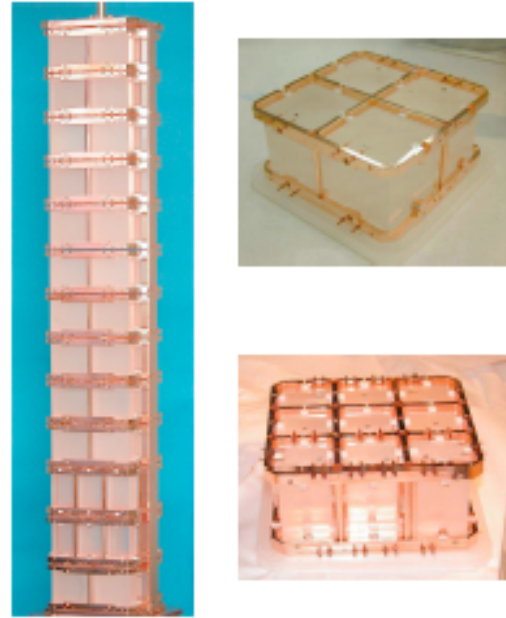


Fig. 1. The CUORICINO Tower and individual 4 and 9 detector modules.

means of a Si resistor of 50-100 k Ω , attached to each bolometer and acting as a heater. Heat pulses are periodically supplied by an ultra-stable calibrated pulser [54] specially designed for the purpose. This sends a calibrated voltage pulse to the Si resistor. This pulse has a time duration very much shorter than the typical thermal response of the detector [44]. The Joule dissipation from the Si resistor produces heat pulses in the crystal almost indistinguishable from those from γ -rays used as calibration lines. The heater pulses are produced with a frequency of about one in every 300 seconds in each of the CUORICINO bolometers. Any variation in the voltage amplitude recorded from the heater pulses indicates that the gain of that bolometer has changed. The heater pulses are used to measure (and later correct offline) for the gain drifts. Two other pulses, one at lower and one at higher energies, are sent to the same resistors with much lower frequency. The former is used to correct threshold stability, and the latter to check the effectiveness of the gain stability correction.

The tower is mechanically decoupled from the cryostat to avoid heating due to vibrations. The tower is connected through a 25 mm copper bar to a steel spring fixed to the 50 mK plate of the refrigerator. The temperature stabilization of the tower is made by means of a thermistor and a heater glued to onto it. An electronic channel is used for a feed back system [55]. The entire setup is shielded with two layers of lead of 10 cm minimum thickness each. The outer one is made of common low radioactivity lead, the inner layer of special lead with a measured content of 16 ± 4 Bq/kg in ^{210}Pb . The electrolytic copper of the refrigerator thermal shields provides an additional shield with a minimum thickness of 2 cm. An external 10 cm layer of borated polyethylene was installed to reduce the background due to environmental neutrons.

The detector is shielded against the intrinsic radioactive contamination of the dilution unit materials by an internal layer of 10 cm of Roman lead (^{210}Pb activity < 4 mBq/kg [49]), located inside of the cryostat immediately above the tower of the array. The background from the activity in the lateral thermal shields of the dilution refrigerator is reduced by a lateral internal shield of Roman lead that is 1.2 cm thick. The refrigerator is surrounded by a Plexiglas anti-radon box flushed with clean N_2 from a liquid nitrogen evaporator and is also enclosed in a Faraday cage to eliminate electromagnetic interference.

The array was cooled down to approximately 8 mK with a temperature spread of ~ 1 mK among the different detectors. Routine calibrations are performed using two wires of thoriated tungsten inserted inside the external lead shield in immediate contact with the outer vacuum chamber (OVC) of the dilution refrigerator. This calibration, normally lasting one to two days, is performed at the beginning and end of each run, which lasts for approximately two-three weeks.

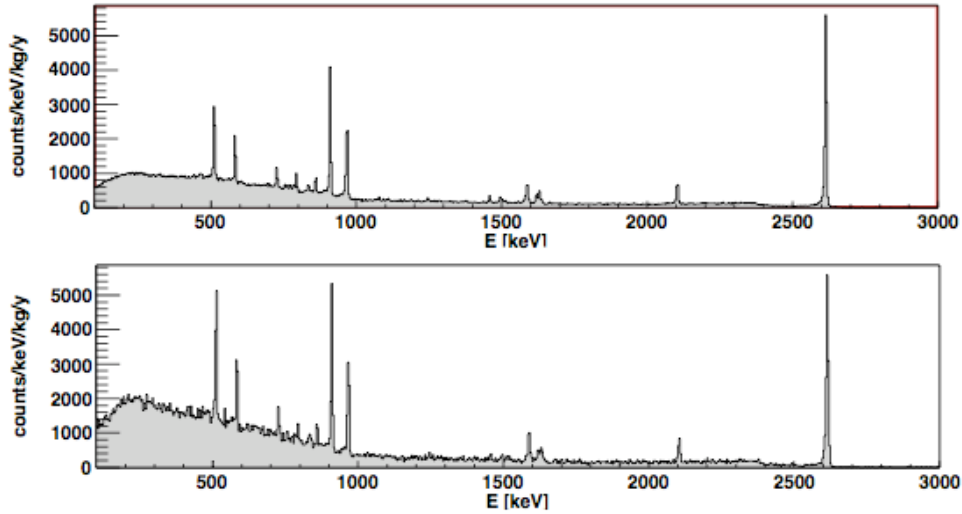


Fig.2. Calibration spectra with a ^{232}Th source in the $5\times5\times5\text{ cm}^3$ detectors (upper), and $3\times3\times6\text{ cm}^3$ (lower).

The CUORICINO array was cooled down at the beginning of 2003. However, during this operation electrical connections were lost to 12 of the 44 detectors of $5\times5\times5\text{ cm}^3$, and to one of the $3\times3\times6\text{ cm}^3$ crystals. Thermal stresses had broken the electrical connections on their thermalizer stages that allow the transition in temperature of the electric signals in various steps from the detectors to room temperature. When the cause of the disconnection was found, new thermalizer stages were fabricated and tested at low temperature. However, since the performance of the remaining detectors was normal, and their total mass was $\sim 30\text{ kg}$, warming of the array and rewiring were postponed for several months while collecting $0\nu\beta\beta$ -decay data. At the end of 2003, CUORICINO data acquisition was stopped and the system was warmed to room temperature and new thermalizer stages were substituted for the broken ones. During this operation, the tower was kept enclosed in its copper box to prevent possible recontamination of the detectors. As a consequence, two detectors whose disconnections were inside of the box were not recovered. The same was true for one of the small central detectors whose Si resistor was electrically disconnected inside the box. In the middle of 2004, CUORICINO was cooled down and data collection began again.

V. DATA ACQUISITION AND ANALYSIS

The signals coming from each bolometer are amplified and filtered with a six-pole Bessel low-pass filter and fed to a 16-bit ADC. The signal is digitized with a sampling time of 8 ms, and a circular buffer is filled. With each trigger pulse, a set of 512 samples is recorded to disk; accordingly, the entire pulse shape is stored for offline analysis. Each channel (bolometer) has a completely independent trigger and trigger threshold, optimized according to the bolometer's typical noise and pulse shape. Starting with run number 2, the CUORICINO data acquisition (DAQ) now has a software trigger that implements a “debounce” algorithm to reduce spurious fast signal triggering. The trigger is ready again within a few tens of ms, a delay due to the debounce time. Therefore, most of the pile-up events are re-triggered. The trigger efficiency above 100 keV was evaluated as $99\pm 1\%$ by checking the fraction of recorded pulser signals. The offline

analysis uses an Optimal Filter technique [44] to evaluate the pulse amplitudes and to compare pulse-shapes with detector response function. Non-particle events are recognized and rejected on the basis of this comparison. Pile-up pulses are identified and correctly dealt with by taking into account that the bolometers act in parallel. In any case, the pile-up fraction during the search for $0\nu\beta\beta$ -decay is completely negligible given the low trigger rate from signals above threshold. The pile-up probability on the rise time, the one most difficult to deal with, is about 0.01%, while that on the entire sampling window is quite a bit higher, $\sim 0.4\%$. However, that is easily identified and the pile-up pulses are rejected. The real pulse amplitudes are then corrected using the variation in the gain measured with the heat pulses from the Si resistors. Finally, spectra are produced for each detector.

Any type of coincidence cut can be applied to the data written to disk, before the creation of the final spectra, depending on the specific analysis desired. In the case of $\beta\beta$ -decay analysis, anticoincidence spectra are used, and in this case, only “good” pulses from a single bolometer are selected, and only if no other bolometer triggered within a time window of ~ 50 ms. This allows the rejection of background counts from gamma rays that Compton scatter in more than one bolometer, for example. The probability of accidental coincidences over the entire detector is negligible ($< 0.6\%$).

VI. SOURCE CALIBRATION AND DETECTOR PERFORMANCE

The performance of each detector is periodically checked during the routine calibration with the ^{232}Th gamma rays from the thoriated calibration wires. The more intense gamma ray peaks visible in the calibration spectra are used to make the spectra linear. The γ -ray lines used are those at: 511, 583, 911, 968, 1588, and 2615 keV, and the single escape peak of the 2615 keV gamma ray at 2104 keV. The resulting amplitude vs energy relationship is fitted to the calibration data, and all pulse amplitudes are converted into energies. The dependence of the amplitude on energy is parameterized with a second order log-polynomial for which the parameters were obtained from the calibration data. The selection of the functional form was established by means of simulation studies based on a thermal model of the detectors. These calibration data are also used to determine the energy resolution of each bolometer. Data sets are collected for two to three weeks, separated by radioactive-source calibrations. The data collected by a single detector in this short time does not have the statistical significance to show the background gamma ray lines because of the very low counting rates. Any control of the energy resolution, and on the stability of the energy calibration, must rely on the heater pulses, and on the initial and final source calibration measurements.

Double-beta decay data collected with each detector during a single data collection period are rejected if any of the following criteria are not fulfilled:

1. The position of the 2615 keV background line in the decay of ^{208}Tl , in the initial and the final source-calibration measurements must differ by less than 1/3 of the measured FWHM of the 2615 keV line for that detector.
2. The energy resolution of the 2615 keV lines in the initial and final energy calibration measurements must be stable within 30%.

3. The energy position corresponding to the heater lines during the entire data collection period for that data set must be stable to within 1/3 of the characteristic FWHM for that detector.

4. The energy resolution, measured with the heater pulses, for that entire data collection period must be stable within 30%.

Whenever any of these criteria is not fulfilled, the data from that detector are not included in the $\beta\beta$ -decay data set. The amount of data discarded by not fulfilling all four criteria, is approximately 17%.

In both runs, the measured detector performances appear to be excellent; the average FWHM resolutions during the calibration measurements are 7 and 9 keV, for the 5x5x5 cm³ and 3x3x6 cm³ detectors respectively, in the energy region around 2530 keV. The spread in the FWHM is about 2 keV in both cases. The smaller detectors have somewhat worse resolution on average, while they also exhibit a very important non-linearity. When the calibration spectra from all of the larger and smaller detectors are summed together, the summed spectrum resembled that of a single large detector as shown in Figure 3.

VII. DOUBLE-BETA DECAY RESULTS

The $0\nu\beta\beta$ -decay measurements began in April 2003. After the long down period between runs 1 and 2 to recover the lost electrical connections, CUORICINO was restarted in May 2004. A second interruption was required to remove the malfunctioning helium liquefier used to automatically refill the main bath of the dilution refrigerator. There were also short interruptions for routine maintenance of the 17-year old refrigerator. Excluding the two long, and several short, interruptions, the duty cycle was very satisfactory, not withstanding the fact that 15 to 20% of the live time is necessary for calibration.

The three spectra corresponding to large (5x5x5 cm³) detectors and the smaller natural and (3x3x6 cm³) enriched detectors are all three kept separate because of the different detection efficiencies for $\beta\beta$ -decay events, and also because of their different background counting rates. For similar reasons, the spectra of the two runs are treated separately. Because the comparison of run-1 and run-2 spectra do not show any statistically significant difference, it was concluded that no recontamination of the detector took place when the cryostat was opened to air during the interruption between runs 1 and 2. The full data set used in this analysis has a total effective exposure of 11.83 kg y of ¹³⁰Te for the entire array.

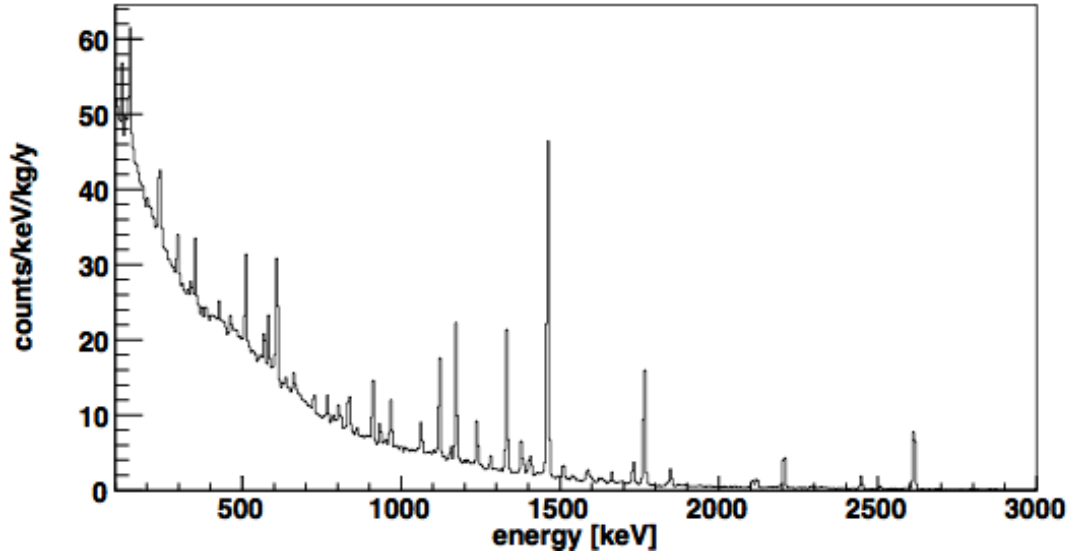


Figure 3a. The sum spectrum of the background from the 5x5x5 cm³ detectors, from both runs, to search for $0\nu\beta\beta$ -decay

The full summed spectrum, shown in Fig. 3a, clearly exhibits the γ -ray line from the decay of ^{40}K , and those from the ^{238}U and ^{232}Th chains. Also visible are the lines of ^{121}Te , $^{121\text{m}}\text{Te}$, $^{123\text{m}}\text{Te}$, $^{125\text{m}}\text{Te}$ and $^{127\text{m}}\text{Te}$, and those of ^{57}Co , ^{58}Co , ^{60}Co , and ^{54}Mn , due to cosmogenic activation of the tellurium and the copper frame. The correct positions and widths of the peaks in the sum spectrum demonstrate the effectiveness of the calibration and linearization of the spectra. The accuracy of calibration in the $0\nu\beta\beta$ -decay region was evaluated to be of about ± 0.4 keV.

The average background counting rates in the region of $0\nu\beta\beta$ -decay are: 0.18 ± 0.01 , and 0.20 ± 0.04 counts per kg, per keV, per year, for the 5x5x5 cm³ and 3x3x6 cm³ crystals, respectively. The sum background spectrum from about 2280 to 2790 keV, of the 5x5x5 cm³ and 3x3x6 cm³ crystals, is shown in Fig. 3b.

The energy resolution for the complete data set was computed from the full width at half maximum (FWHM) of the 2615 keV background γ -ray line in the decay of ^{203}Tl at the end of the thorium chain. The results are 8 keV for the forty operating 5x5x5 cm³ crystals, and 12 keV for the eighteen 3x3x6 cm³ crystals. Clearly visible is the peak at about 2505 keV due the summing of the 1332.50-1172.24 keV γ -ray cascade in the decay of ^{60}Co . This is 25.46 keV, i.e., more than 4 sigma from the energy window of the $0\nu\beta\beta$ -decay of ^{130}Te , and would make a negligible contribution to the region under the expected $0\nu\beta\beta$ -decay peak .

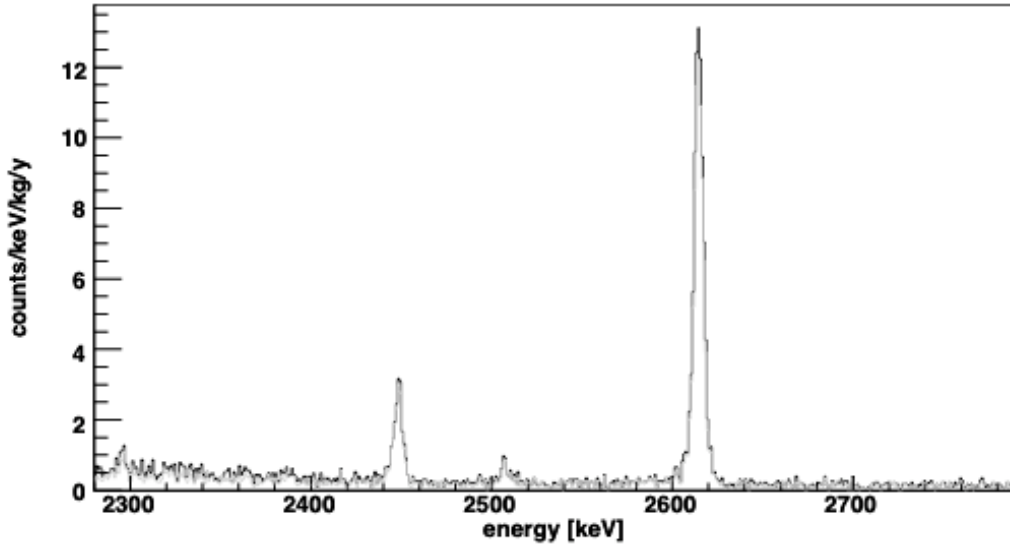


Figure 3b. The summed background spectrum in the ~ 600 keV region of interest including the $0\nu\beta\beta$ -decay energy 2530.3 ± 2.0 keV.

The details of the operating conditions and parameters of the two CUORICINO data collection periods is given in Table 2. The total usable exposure for Run I + Run II is 11.83 kg.y of ^{130}Te . The event detection efficiencies were computed with Monte-Carlo simulations; they are 0.863 and 0.845 for the large and small crystals, respectively. From the above exposure data we compute: $\ln 2 \times N_L \times \varepsilon_L \times t = 2.809 \times 10^{25}$ y, for the large and $\ln 2 \times N_S \times \varepsilon_S \times t = 4.584 \times 10^{24}$ y for the small crystals. Here, ε is the detection efficiency, and $N_{L,S}$ is the number of ^{130}Te nuclei in the large and small detectors respectively.

The $\beta\beta$ -decay half-life limit was evaluated using a Bayesian approach. The peaks and continuum in the region of the spectrum centered on the $\beta\beta$ -decay energy were fit using a maximum likelihood analysis. The likelihood functions of six spectra (the sum spectra of the three types of crystals in the two runs) were combined allowing for a different background level for each spectrum, and a different intensity of the 2505-keV ^{60}Co sum peak. Other free parameters are the position of the ^{60}Co peak and the number of counts under a peak at the $\beta\beta$ -decay energy. The same procedure is used to evaluate the 90% C.L. limit to the number of counts present in the $\beta\beta$ -decay peak.

Assuming Poisson statistics for the binned data, the fit procedure was formulated in terms of the likelihood chi-square analysis as described in the following equation:

$$\chi_L^2 = 2 \sum_{j=1}^6 \sum (y_{i,j} - n_{i,j} + n_{i,j} \ln(n_{i,j} / y_{i,j})),$$

where j indicates the j^{th} spectrum, n_{ij} is the number of events in the i^{th} bin of the j^{th} spectrum and y_{ij} is the number of events predicted by the fit model.

Fit parameters were estimated minimizing the χ_L^2 , while limits were obtained, after proper renormalization, considering the χ_L^2 distribution in the physical region. The response function for each spectrum is assumed to be a sum of symmetric gaussian functions, each having the typical energy resolution of one of the detectors summed in that spectrum. The experimental uncertainty in the transition energy is considered by means of a quadratic (gaussian) term in the above equation. Considering the region between 2575 and 2665 keV and assuming a flat background a negative effect of -13.9 ± 8.7 is found, while the resulting upper bound on the number of candidate events in the $\beta\beta$ -decay peak is 10.7 to the 90% C.L. These values are normalized to a hypothetical sum spectrum of the entire statistical data set in which each of the six spectra are weighted according to the corresponding exposure, geometric efficiency, and isotopic abundance. Once converted into a lower limit on the half-life, the result is at $T_{1/2}^{0\nu}(^{130}\text{Te}) \geq \ln 2 \{N_t \varepsilon_t + N_s \varepsilon_s\} t / n(90\%CL) = (3.268 \times 10^{25} / 10.7) y = 3.0 \times 10^{24} y$.

The dependence of the value of the limit on systematic uncertainties that arise from the method of analyzing the data was investigated in detail. These uncertainties reside in the dead time, in the energy calibration, and in the Q-value, and in the background spectral shape. The main factor influencing the limit turned out to be the uncertainty in the background spectral shape. For example, changing the degree of the polynomial used to fit the background in the $\beta\beta$ -decay region from 0 to 2, as well as the selection of the energy window used in the analysis, can vary the bound from 2.5 to $3.3 \times 10^{24} y$.

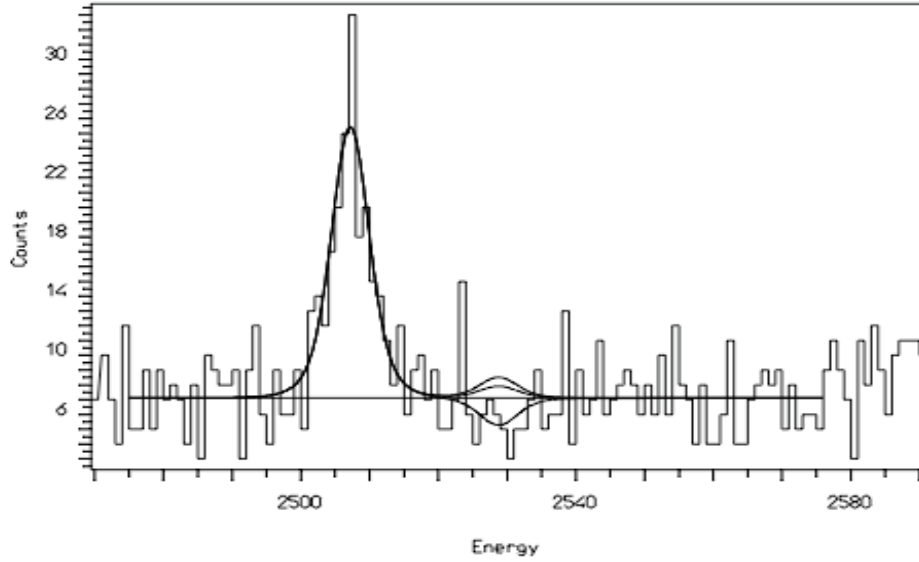


Figure 4. A close-in view of the total background spectrum from 2470 to 2590 keV. Clearly visible is the sum peak at 2505.68 keV due to the sum of the 1173.21 and 1332.47 keV gamma-ray cascade in the decay of ^{60}Co . This activity is attributed to the ^{60}Co in the copper frames generated by cosmic ray neutrons while the frames were above ground. There is an obvious small dip in the data at the expected $\beta\beta$ -decay energy, 2530.3 ± 2.0 keV. The solid lines are the best fit to the region, and the bounds (68% and 90%) on the number of candidate $\beta\beta$ -decay events.

VIII. NUCLEAR STRUCTURE ISSUES

There is one theoretical viewpoint that holds that the required model space for ^{130}Te is still very large for reliable shell model calculations and must be severely truncated. Accordingly, the Quasi-Particle Random Phase Approximations (QRPA) have been commonly used [58-77]. The results from these calculations, from author to author had, until very recently, differed significantly for the same nucleus. In Table 3, only the results from references [61,72] differ significantly from the other 13; they are from the largest matrix elements. QRPA calculations depend, for example, on the single-particle space included, on the interaction potential, and on the method used for including the short-range correlations in the particle-particle interactions, and on the value of the axial vector coupling constant, g_A , used. Some use the value 1.245 obtained from the neutron decay lifetime, and some use the value 1.00, quenched by virtual-pion interactions in finite nuclei. In the QRPA approach, the particle-particle interaction is fixed by a parameter, g_{pp} , which is derived in various ways by different authors. A very recent paper by Rodin et al., gives a detailed assessment of the uncertainties in QRPA calculations of

$0\nu\beta\beta$ -decay matrix elements, and explains many of the reasons for the disagreements between the various authors over the years [59,60]. The numerical values given in these articles were corrected in a later erratum [78]. In Table 3 we list the values of $\langle m_\nu \rangle$ corresponding to $T_{1/2}^{0\nu}(^{130}\text{Te}) \geq 3.0 \times 10^{24} \text{ y}$, derived using the calculations of various authors. More details are discussed later, including the results from recent shell model calculations.

As stated earlier, the interpretation of the half-life data, to extract the corresponding effective Majorana mass of the electron neutrino, requires the calculation of the nuclear matrix element factor, $(M_F^{0\nu} - (g_A/g_F)^2 M_{GT}^{0\nu})$, in equation (2). In the nuclei that are the best candidates for $0\nu\beta\beta$ -decay experiments, this is not straightforward because they have many valence nucleons in the model space. To create a tractable shell-model calculation for these heavy nuclei, ^{130}Te for example, it is necessary to truncate the model space to the point that the results in the past have not been reliable. Accordingly, schematic models are employed. As stated above, QRPA has become the standard approach for both $2\nu\beta\beta$ - and $0\nu\beta\beta$ -decay. The results calculated with QRPA, however, depend on the selection of a number of parameters, and the fact that different authors select the parameters in various ways, has resulted in large differences in the resulting matrix elements as discussed in reference [60].

In Table 3, we list 14 different values of $\langle m_\nu \rangle$ derived with QRPA and with renormalized QRPA, (RQRPA), corresponding to $T_{1/2}^{0\nu}(^{130}\text{Te}) = 3.0 \times 10^{24} \text{ y}$, and also the recent shell-model calculations of Caurier et al. [78]. From the table it is clear that the different ways of applying the same basic model has lead to a spread in the resulting matrix elements, and hence in the corresponding value of $\langle m_\nu \rangle$, of a factor of three [60-73]. This corresponds to differences of a factor of nine in the predicted half-life for a given value of $\langle m_\nu \rangle$, if all calculations are given the same weight. This, however, cannot be justified. It should be recognized that progress must certainly have been made over time, and that calculation techniques, as well as computational power have made significant progress over the years.

In their recent article, Rodin, Simkovic, Faessler, and Vogel [60], give detailed discussions of how the choices of various parameters in similar models can lead to such discrepancies. These are: the gap of the pairing interactions, the use of (Renormalized) RQRPA that partially accounts for the violation of the Pauli principle in the evaluation of the two-fermion commutators, the nucleon-nucleon interaction potential, the strength of the particle-hole interactions of the core polarization, the size of the model space, and the strength of the particle-particle interaction, parameterized by the quantity, g_{pp} . The matrix elements of the virtual transitions through states with $J^\pi = 1^+$ in the intermediate nucleus are extremely sensitive to the value of g_{pp} , which makes $2\nu\beta\beta$ -decay matrix elements also very sensitive to it because this decay mode only proceeds through 1^+ intermediate states. On the other hand, $0\nu\beta\beta$ -decay also proceeds via higher multipoles through states of higher spin. These transitions are found to be far less sensitive to the value of g_{pp} . For this reason, Rodin et al., select the value of g_{pp} that makes the

calculation of the $2\nu\beta\beta$ -decay half-life agree with the experimental value. In addition, some calculations are greatly simplified by using an average energy in the denominator of the second order matrix element expression, and the sum over the intermediate states is done by closure. In some calculations, the value 1.25, of the axial-vector coupling constant, g_A , obtained from muon decay is used which commonly leads to a value of the Gamow-Teller strength typically larger than the measured value. To ameliorate this situation, a quenched value $g_A = 1.00$ is used. In calculated rates of $2\nu\beta\beta$ -decay, which proceed only through $J^\pi = 1^+$ states, this results in a factor of 2.44 reduction in the rate. Using the technique of Rodin et al., [60], the choice of $g_A = 1.00$ reduces the rate by between 10 to 30%.

Another serious difference between some of the $0\nu\beta\beta$ -decay calculations is due to the treatment of the short-range correlations in the nucleon-nucleon interactions. Finally, it was first pointed out by Simkovic et al., [67], that including the momentum dependent higher order terms of the nucleon current typically result in a reduction in the calculated value of the $0\nu\beta\beta$ -decay matrix element by about 30%. These were included in the calculations of reference [60].

In recent paper by Alvarez et al., [74], a QRPA formalism for $2\nu\beta\beta$ -decay in deformed nuclei was presented. A significant reduction in the matrix elements was observed in cases in which there was a significant difference in the deformations of the parent and daughter nuclides. Exactly how this would affect $0\nu\beta\beta$ -decay is not yet clear.

In general, however, the paper by Rodin et al., [60], represents a detailed study of the various factors that cause the large variations in the nuclear matrix elements of $0\nu\beta\beta$ -decay calculated by different authors over the years, and must be taken seriously. The procedure of Rodin et al. [58-60] has the attractive feature that it gives a straightforward prescription for selecting the very important particle-particle parameter, g_{pp} . However, Civitarese and Suhonen (referred to as the *Jyväskylä* group) have given strong arguments in favor of using single β^\pm -decay and electron capture data for this purpose, while giving arguments against using experimental $2\nu\beta\beta$ -decay half lives [64]. They argue that only states with spin and parity 1^+ can be the intermediate states involved in $2\nu\beta\beta$ -double-beta decay, and that in the neutrino-less process these states play a minor role. They show that the higher spin states play a dominant role in $0\nu\beta\beta$ -decay. The *Jyväskylä* group recently presented a preprint in which they show that the effects of short-range correlations have been significantly overestimated in the past [75-76]. Accordingly, their matrix elements originally gave a very different picture of the of the physics impact of the CUORICINO data presented in this paper. However, recently there have been some very important developments discussed below.

IX. RECENT DEVELOPMENTS IN QRPA CALCULATIONS

We adopt the position that the large dispersion in values in the nuclear matrix elements implied by the values in Table 3 does not reflect the true state of the art. Instead,

we assume that over the past ten or so years, there has been significant progress in understanding the key theoretical issues, as well as a large increase in available computational power. Until the time of this writing, however, two of the recent extensive theoretical treatments of the $0\nu\beta\beta$ -decay matrix elements disagreed significantly, and in particular in the case of ^{130}Te . The relevant nuclear structure factors, F_N , from the *Jyväskylä* and *Tübingen* groups for $g_A = 1.25$ were: $F_N(^{130}\text{Te}) = 1.20 \pm 0.27 \times 10^{-13} \text{ y}^{-1}$ of Rodin et al., [60], and $F_N(^{130}\text{Te}) = 5.13 \times 10^{-13} \text{ y}^{-1}$ of Civitarese and Suhonen [64].

However, on June 22nd 2007 an erratum was submitted by Rodin et al., [77] that made major corrections to Table 1 of reference [60]. A coding error was discovered in the computation of the short-range correlations that, for example, increased the predicted $0\nu\beta\beta$ -decay rate of ^{130}Te by a factor of 4.03. Their corrected value of the nuclear structure factor of ^{130}Te , for example, is now: $F_N(^{130}\text{Te}) = 4.84^{+1.30}_{-0.64} \times 10^{-13} \text{ y}^{-1}$. This is in good agreement with the above value given by Civitarese and Suhonen. However, there is still a smaller remaining disagreement between these two groups concerning the application of the short-range correlations. Rodin et al., used a Jastrow-correlation function, which has subsequently been shown by Kortelainen et al., [75] to overestimate the effects of short-range correlations, and hence results in an excessive reduction in the nuclear matrix elements.

Since the original draft of the present article, Kortelainen et al., [76] have updated the calculations of Civitarese and Suhonen. They extended their model space, for the cases of ^{116}Cd , $^{128,130}\text{Te}$ and ^{136}Xe , to include: the 1p-0f-2s-1d-0g-2p-1f-0h single particle orbitals, calculated with a spherical Coulomb-corrected Woods-Saxon potential. They give a complete discussion of their method of fixing the parameters of their Hamiltonian. In this treatment they fix particle-particle parameter g_{pp} of the pnQRPA, using the method of Rodin et al., [58-60], namely with the experimentally measured $2\nu\beta\beta$ -decay half-lives. In this case, they did not use the Jastrow-correlation function to correct for the short-range correlations, but rather they employ a “unitary correlation operator method” (UCOM), which in the case of ^{130}Te increases the matrix element by a factor of 1.38 over that calculated with the Jastrow correlation function. Their new values for the nuclear structure function are:

$$F_N(^{130}\text{Te})_{g_A=1.25} = 7.47 \times 10^{-13} \text{ y}^{-1}$$

$$F_N(^{130}\text{Te})_{g_A=1.00} = 4.93 \times 10^{-13} \text{ y}^{-1}$$

This is to be compared to the results of the earlier work of Civitarese and Suhonen [64].

In any case, the major disagreements between the *Jyväskylä* and *Tübingen* groups have finally been understood, and the present difference in the predicted $0\nu\beta\beta$ -decay rates of ^{130}Te now differ by a factor of 1.06, whereas the earlier disagreement was by a factor of 4.28. Some remaining differences might well lie in the differing methods of applying the short-range correlations. In any case these recent developments have had a major impact on the present interpretation of the CUORICINO data.

Furthermore, the group of Caurier et al., [78], have recently given new values for these matrix elements from improved nuclear shell model calculations. The shell-model matrix elements are somewhat smaller than those of the recent *Jyväskylä* and corrected *Tübingen* results, and according to their matrix elements, the CUORICINO data imply: $\langle m_\nu \rangle \leq 0.58 \text{ eV}$.

X. CUORICINO AS A TEST OF THE CLAIM OF DISCOVERY

The CUORICINO array is the only operating $0\nu\beta\beta$ -decay experiment, with good energy resolution, that could potentially probe the range of effective Majorana mass, $\langle m_\nu \rangle$, implied by claim of evidence the Klapdor-Kleingrothaus et al., [19,20] of a direct observation. In the 2006 article by Klapdor-Kleingrothaus and Krivosheina (KK&K)[20], the peak in the spectrum centered at $|Q_{\beta\beta}| \approx 2039 \text{ keV}$ is interpreted as the $0\nu\beta\beta$ -decay of ^{76}Ge , consistent with the range: $T_{1/2}^{0\nu}(^{76}\text{Ge}) = \{1.30 - 3.55\} \times 10^{25} \text{ y}$ (3σ). The best-fit value is $(2.23_{-0.31}^{+0.44}) \times 10^{25} \text{ y}$. In this discussion we offer no critique of the claim, but accept it at face value. However, since this claim has been criticized from several points of view [21-23], it is interesting to ask if it is feasible to observe a $0\nu\beta\beta$ -decay with this half-life with a $\sim n\sigma$ confidence level (C.L.) with the published parameters of the experiment. Below, we show that the answer is "yes", the experiment could have made the observation in the range of half-lives quoted [20].

It is straightforward to derive an approximate analytical expression for the half-life sensitivity for discovery at a given confidence level that an experiment can achieve. (see Appendix A.) The achievable discovery half-life, when the background rate is non- zero, is expressed as:

$$T_{1/2}^{0\nu}(n_\sigma) = \frac{4.17 \times 10^{26} \text{ y}}{n_\sigma} \left(\frac{\epsilon a}{W} \right) \sqrt{\frac{Mt}{(1+\zeta)b\delta(E)}}. \quad (9)$$

It is more conventional to simply have $b\delta(E)$ in the denominator of the root of equation (9) as prescribed by the Particle Data Book [81]. However, when the background continuum is obtained by a best fit to all peaks and continuum in the region, we choose this alternative approach. In equation (9), n_σ is the desired number of standard deviations of the C.L. (3 for $C.L. = 99.73\%$, for example), ϵ is the event detection and identification efficiency, a is the isotopic abundance, W is the molecular weight of the source material, M is the total mass of the source, ζ is the required signal-to-background ratio, b , is the specific background rate in counts/keV/kg/y, and $\delta(E)$ is the instrumental width of the region of interest related to the energy resolution at the energy of the expected $0\nu\beta\beta$ -decay peak.

The values for these parameters for the Heidelberg-Moscow experiment [17, 19,20] are: $Mt = 71.7 \text{ kg} \cdot \text{y}$, $b = 0.11 \text{ kg}^{-1} \text{ keV}^{-1} \text{ y}^{-1}$, $\epsilon = 0.95$, $a = 0.86$, $W = 76$, and $\delta(E) = 3.27 \text{ keV}$. The number of counts under the identified peak at 2039 keV is 28.75 ± 6.86 . The average value of the background near the region of interest was 11.6 counts, therefore $\zeta \approx 2$. Direct substitution into equation (9) yields:

$$T_{1/2}^{0\nu}(4\sigma, {}^{76}\text{Ge}) = 0.9 \times 10^{25} \text{ y}; T_{1/2}^{0\nu}(3\sigma) = 1.2 \times 10^{25} \text{ y} \quad (10a)$$

Using the less conservative approach with $b\delta(E)$ in the denominator, the predicted half-life sensitivity for a discovery is:

$$T_{1/2}^{0\nu}(4\sigma, {}^{76}\text{Ge}) = 1.6 \times 10^{25} \text{ y}; T_{1/2}^{0\nu}(3\sigma) = 2.13 \times 10^{25} \text{ y} \quad (10b)$$

These are close to the claimed most probable value given in reference [20]. This analysis is independent of the claimed result, with the exception of the determination of the signal to background ratio, ξ . The conclusion is that with the given experimental parameters, this experiment could well have had a discovery potential. Since this analysis does not account for statistical fluctuations, the discovery confidence level could very well fall between 3σ and 5σ . Any criticism of the claim would involve a reanalysis of the data, and the interpretation of the background peaks in the region. This falls outside of the scope of this discussion. Instead we accept the claim at face value, and ask how well the present CUORICINO data confront it, now and in the future after 5 years of running.

First we interpret the half-life, $T_{1/2}^{0\nu}({}^{76}\text{Ge}) = \{1.30 - 3.55\} \times 10^{25} \text{ y}$, in terms of the list of nuclear structure calculations listed in Table 2 of the review of Elliott and Engel [6] for ${}^{76}\text{Ge}$, and Table 3 of this article for ${}^{130}\text{Te}$. In this scenario:

$$T_{1/2}^{0\nu}({}^{76}\text{Ge}) = \{1.30 - 3.55\} \times 10^{25} \text{ y} \Rightarrow \langle m_\nu \rangle = (0.22 - 1.19) \text{ eV} \quad (11)$$

$$T_{1/2}^{0\nu}({}^{130}\text{Te}) \geq 3.0 \times 10^{24} \text{ y} \Rightarrow \langle m_\nu \rangle \leq (0.19 - 0.68) \text{ eV}. \quad (12)$$

At first glance, it would appear that the present CUORICINO bounds really begin to challenge the Heidelberg group's claim. It is, however, more correct to compare the results for both isotopes in the same model one by one as one can do by reference to Table 3. The above analysis only gives a quick look at the situation.

There have been many theoretical calculations of the nuclear matrix elements over the years, and the spread of values has in the past been significant. The recently corrected-QRPA calculations of Rodin et al., [77], those of Civitarese and Suhonen [64], and shell model calculations of Caurier et al., [78], differ by less than about 30%. We have chosen to use these for further analysis of the physics impact of the present CUORICINO data.

Equation (8) can be inverted to obtain the values of the nuclear structure factor, F_N , using the calculated half-lives for $0\nu\beta\beta$ -decay calculated with a given $\langle m_\nu \rangle$ by the authors of the theoretical papers. The resulting values are as follows:

${}^{76}\text{Ge}(g_A = 1.245)$:

$$\begin{aligned} \text{Rodin et al. } F_N &= 1.22_{-0.11}^{+0.10} \times 10^{-13} \text{ y}^{-1}, \\ \text{Caurier et al. } F_N &= 4.29 \times 10^{-14} \text{ y}^{-1} \text{ and} \end{aligned} \quad (13)$$

Civitarese and Suhonen $F_N = 7.01 \times 10^{-14} \text{ y}^{-1}$.

$^{130}\text{Te}(g_A = 1.245)$:

$$\begin{aligned} \text{Rodin et al. } F_N &= 4.84^{+1.30}_{-0.64} \times 10^{-13} \text{ y}^{-1} \text{ (corrected value)} \\ \text{Caurier et al. } F_N &= 2.57 \times 10^{-13} \text{ y}^{-1} \\ \text{Civitarese and Suhonen } F_N &= 5.13 \times 10^{-13} \text{ y}^{-1} \end{aligned} \quad (14)$$

The resulting values and ranges of values of $\langle m_\nu \rangle$ implied by the KK&K data, and by the CUORICINO data are as follows:

$$\begin{aligned} \langle m_\nu \rangle_{kk\&k}^{Rod} &= \{0.23 - 0.43\} \text{ eV} \\ \langle m_\nu \rangle_{cuo}^{Rod} &\leq \{0.38 - 0.46\} \text{ eV} \\ \langle m_\nu \rangle_{kk\&k}^{Civ} &= \{0.32 - 0.54\} \text{ eV} \\ \langle m_\nu \rangle_{cuo}^{Civ} &\leq 0.41 \text{ eV} \\ \langle m_\nu \rangle_{kk\&k}^{SM} &= \{0.41 - 0.68\} \text{ eV} \\ \langle m_\nu \rangle_{cuo}^{SM} &\leq 0.58 \text{ eV} \end{aligned} \quad (15)$$

The results of the analyses with the new corrected matrix elements of Rodin et al., [77], imply that the CUORICINO sensitivity has entered well into the range of values of $\langle m_\nu \rangle$ implied by the claim of KK&K. In the other two analyses, the CUORICINO data also constrain part of the range of values of $\langle m_\nu \rangle$ implied by KK&K.

It is further interesting to try to predict the sensitivity of CUORICINO if it were to continue to operate for a total of 5 years. The three recent calculations of the nuclear matrix elements result in the following predicted decay rates if the Heidelberg claim is correct. In this case, the decay rates would be:

$$\begin{aligned} \tau_{kk\&k}^{-1}(^{76}\text{Ge}) &= \{1.95 - 5.32\} \times 10^{-26} \text{ y}^{-1} \\ \tau_{Rod}^{-1}(^{130}\text{Te}) &= \{0.62 - 2.94\} \times 10^{-25} \text{ y}^{-1} \\ \tau_{Civ}^{-1}(^{130}\text{Te}) &= \{1.43 - 3.89\} \times 10^{-25} \text{ y}^{-1} \\ \tau_{SM}^{-1}(^{130}\text{Te}) &= \{1.17 - 3.19\} \times 10^{-25} \text{ y}^{-1} \end{aligned} \quad (16)$$

Accordingly, we can calculate the number of $0\nu\beta\beta$ -decay counts with 5 years of live-time operation expected in the CUORICINO data consistent with the claim of KK&K. The exposure would be: $Nt\varepsilon = 2.85 \times 10^{26} \text{ y}$, resulting in the following predicted number of real $0\nu\beta\beta$ -decay events:

$$\begin{aligned}
\tau_{Rod}^{-1} N t \epsilon &= \{18 - 84\}_{0\nu\beta\beta} \\
\tau_{Civ}^{-1} N t \epsilon &= \{41 - 110\}_{0\nu\beta\beta} \\
\tau_{SM}^{-1} N t \epsilon &= \{33 - 91\}_{0\nu\beta\beta}
\end{aligned} \tag{17}$$

These counts would be superimposed on an expected background of 35 to 39 counts per keV in the 8 keV region of interest centered at 2530 keV.

The constraints placed by the current CUORICINO data might favor the lower numbers in the ranges above. This would make it more challenging for CUORICINO to confirm the discovery claim of KK&K, and renders it almost impossible to rule it out with a significant level of confidence. The solution to this problem is the construction and operation of the proposed first tower of CUORE, called CUORE-0, and later the complete CUORE Experiment.

XI. THE PROPOSED CUORE EXPERIMENT

The proposed CUORE detector comprises 19 towers of TeO₂ bolometers, very similar to the CUORICINO tower [28]. Each will house 13 modules of four 5x5x5 cm crystals with masses of ~750 g. CUORE will contain ~200 kg of ¹³⁰Te. The 988 bolometers will have a total detector mass of ~750 kg and will operate at 8-10 mK. An intense research and development program is underway to reduce the background to 0.01 counts/keV/kg/y. Thus far a reduction has been achieved that has reached within a factor of 2.4 of this goal in the region of 2030 keV, the $|Q|$ -value for the $0\nu\beta\beta$ -decay of ¹³⁰Te. With this background, CUORE would reach a sensitivity of $\sim T_{1/2}^{0\nu}({}^{130}\text{Te}) \approx 2.1 \times 10^{26}$ y in 5 years. The secondary goal is to achieve a background level of 0.001 counts /keV/kg/y. This would allow a half-life sensitivity of $T_{1/2}^{0\nu} \approx 6.5 \times 10^{26}$ y.

The associated sensitivities in the effective Majorana mass of the electron neutrino, $\langle m_\nu \rangle$, would be :

$$\begin{aligned}
\langle m_\nu \rangle_{Rod.} &= \{0.026 - 0.031\} eV, \\
\langle m_\nu \rangle_{Civ.} &= 0.028 eV, \\
\langle m_\nu \rangle_{SM} &= 0.040 eV.
\end{aligned} \tag{18}$$

It is also obvious from equation (9) that the half-life sensitivity is directly proportional to the abundance, a , of the parent $\beta\beta$ -decay isotope. Accordingly, enriching the detectors of CUORE from 33.8% in ¹³⁰Te to 90%, CUORE would achieve the same sensitivity with a background of 0.01 counts/keV/kg/y as it would with natural abundance Te and a background of 0.0014 counts/keV/kg/y. Support for an R&D program, to determine the feasibility and cost of isotopically enriching CUORE, has recently been funded. In addition, the CUORE collaboration has a rigorous R&D program to improve the energy resolution from an average of 8keV, as it is in CUORICINO, to 5keV. If in the end, CUORE does achieve the background of 0.001

counts/keV/kg/y, in addition is enriched, has an average energy resolution of 5keV, it could reach a half life sensitivity of 2.5×10^{27} y in 10 years. In this case the sensitivities become:

$$\begin{aligned}\langle m_\nu \rangle_{Rod.} &= \{13-16\} meV, \\ \langle m_\nu \rangle_{Civ} &= 14 meV, \\ \langle m_\nu \rangle_{SM} &= 20 meV.\end{aligned}\tag{19}$$

This brings the sensitivity into the normal hierarchy region, which exceeds the goals of some of the other next generation experiments. It is possible to proceed as planned with a natural abundance version of CUORE, and then the bolometers could be replaced with those isotopically enriched in ^{130}Te . This would of course increase the half-life reach by a factor of 2.5 for an enrichment of 85%.

XIII. SUMMARY AND CONCLUSIONS

The CUORICINO detector is an array of 62 TeO_2 bolometers operating at a temperature of about $8mK$. It has a total mass of $40.7kg$ of TeO_2 , containing $11kg$ of ^{130}Te . It has operated for a total exposure of $N(^{130}\text{Te})t\varepsilon = 5.47 \times 10^{25}$ y, resulting in a lower bound, $T_{1/2}^{0\nu}(^{130}\text{Te}) \geq 3.0 \times 10^{24}$ y. The corresponding upper bound on the effective Majorana mass of the electron neutrino, $\langle m_\nu \rangle$, using the corrected nuclear structure calculations of Rodin et al., [77] is $\langle m_\nu \rangle \leq (0.38-0.46)eV$, while using those of Civitarese and Suhonen [64] yields $\langle m_\nu \rangle \leq 0.47eV$. With the very recent shell model calculations [78], the CUORICINO data imply $\langle m_\nu \rangle \leq 0.58eV$. In all cases, the present CUORICINO data probe a significant portion of the range of the half life measured by KK&K. In the case that the Heidelberg claim is correct, the nuclear structure calculations of ref. [77] imply that after 5 years of live time, CUORICINO would detect $\{18-84\}, 0\nu\beta\beta$ -decay events, while those of ref. [64] imply it would detect $\{41-110\}$ events, and those of ref. [78] imply it would detect $\{33-91\}$ $0\nu\beta\beta$ -events. In all cases, these counts would appear in Gaussian peaks with $FWHM = 8keV$, superimposed on an average background of 29 counts keV^{-1} .

In any case, the current results imply that the continued operation of CUORICINO is very important since it represents the only possibility of testing the claim of evidence of $0\nu\beta\beta$ -decay for the next 5 to 10 years.

ACKNOWLEDGEMENTS

The CUORICINO Collaboration owes many thanks to the Directors and their Staffs of the Laboratori Nazionali del Gran Sasso over the years of the development, construction and operation of CUORICINO, and to the technical staffs of our Laboratories. The experiment was supported by the Istituto Nazionale di Fisica Nucleare

(INFN), the Commission of the European Community under Contract No. HPRN-CT-2002-00322, by the U.S. Department of Energy under Contract No. DE-AC03-76-SF00098, and DOE W-7405-Eng-48, and by the National Science Foundation Grants Nos. PHY-0139294 and PHY-0500337. We also wish to thank the following colleagues for their help and advice: Juoni Suhonen, Osvaldo Civiterese, Petr Vogel, Amand Faessler, Vadim Rodin, and Fedor Simkovic, and Fernando Ferroni.

APPENDIX A

An approximate expression for estimating the $0\nu\beta\beta$ -decay half-life at which a given experiment can achieve discovery at the confidence level corresponding to n_σ σ , can be derived by reference to Figure (A-1). Let “C” be the total number of counts found in the region of the expected $0\nu\beta\beta$ -decay peak; let “B” be the total number of background counts in the same energy interval, $\delta(E)$. For the number of real $0\nu\beta\beta$ -decay events to have a statistical significance of n_σ , then the following must be true: $C - B = n_\sigma \sqrt{C}$. In the usual case where $B \neq 0$, a desired signal to background ratio, $\xi \equiv (C - B)/B$, can be chosen; hence $C = (1 + \xi)B$. The usual expression for the corresponding half-life can be written in terms of these parameters as:

$$T_{1/2}^{0\nu}(n_\sigma) = \frac{(\ln 2)Nt\varepsilon}{n_\sigma \sqrt{(1 + \xi)B}}, \quad (\text{A-1})$$

where N is the total number of parent nuclei, ε is the total detection efficiency, and t is the live time of the data collection. The number of parent nuclei can be written in terms of, M , the total mass of the source (in an oxide for example), as follows: $N = (10^3 \text{ g/kg/Wg/mole}) \cdot (A_0 \text{ at/mole}) \cdot a(\text{abundance}) \cdot M \text{ kg}$. Substituting these values, and expressing the background in terms of the background rate, $B = bM\delta(E)t$, where $b = (\text{counts/keV/kg/y})$, the expression is written:

$$T_{1/2}^{0\nu}(n_\sigma) = \frac{4.17 \times 10^{26}}{n_\sigma} \left(\frac{a\varepsilon}{W} \right) \sqrt{\frac{Mt}{(1 + \xi)b\delta(E)}}. \quad (\text{A-2})$$

Of course in the case of zero background, equation (A-1) is used, and the quantity $n_\sigma(1 + \xi)B$ is replaced by the number of real events in the peak ($C - B$). In case there are no real or background events i.e., $C = B = 0$, the denominator of (A-1) is replaced by the usual quantity, $\ln\{1/(1 - C.L.)\}$, which is 2.3, (90% C.L.) for example, and $T_{1/2}^{0\nu}$ becomes an experimental lower limit. In equation A-2, we use the fluctuation in the real events instead of that of the background because in these experiments the background level used is that of a best fit curve to the background in the region, and the fluctuation is a fitting error and is much smaller than the statistical fluctuations in the region of interest.

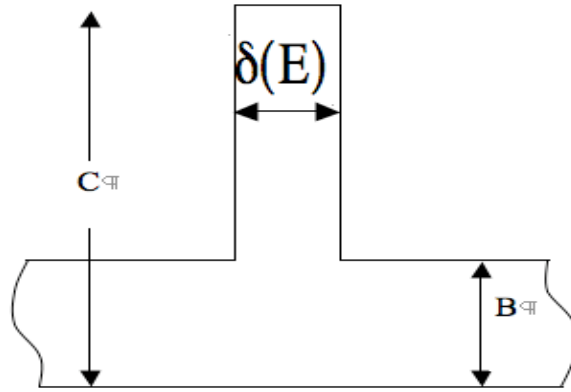


Figure (A-1). Sketch of a peak on a continuum; C and B are actually the total number of counts and total background in the energy interval $\delta(E)$, respectively.

REFERENCES

- [1] M. Goeppert-Mayer, Phys. Rev. **48**, 512 (1935).
- [2] Ya. B. Zel'dovich, Yu. Luk'yanov, and Ya. A. Smorodinski, Usp. Fiz. Nauk. **54**, 361 (1954);
- [3] H. Primakoff and S.P. Rosen, Rep. Prog. Phys. **22**, 121 (1959; Ann. Rev. Nucl. Part.Sci. **31**,145 (1981); W.C. Haxton and G.J. Stephenson Jr., Prog. Nucl. Part. Phys.,**12**, 409 (1984).
- [4] Yuri Zdesenko, Rev. Mod. Phys. **74**, 663 (2002); F.T. Avignone III, G.S. King III, and Yu. G. Zdesenko, New Journal of Physics, **7**, 6 (2005).
- [5] S.R Elliott and P. Vogel, Annu. Rev. Part. Sci. **52**, 115 (2000).
- [6] S.R. Elliott and J. Engel, J. Phys.G: Nucl. Part. Phys.**30R**, 183 (2004);, F.T. Avignone III, S.R. Elliott, and J. Engel, Rev. Mod. Phys. (in press); arXiv:0708.1033 [nucl-ex].
- [7] T. Kajita and Y. Totsuka, Rev. Mod. Phys. **73**, 85 (2001). (See references therein).
- [8] B.T. Cleveland et al., Astrophys. J. **496**, 505 (1998). (See references therein).
- [9] J.N. Abdurashitov et al, (The Sage Collaboration), J. Exp. Theor. Phys. **95**, 181 (2002).
- [10] W. Hampel et al., (The GALLEX Collaboration), Phys. Lett. B **447**,127 (1995).
- [11] S. Fakuda et al., (The SuperKamiokande Collaboration), Phys. Rev. Lett. **86**, 5651 (2001); **86**, 5656 (2001).
- [12] Q.R. Ahmad et al., (The SNO Collaboration), Phys. Rev. Lett. **87**, 071301 (2001).
- [13] J.N. Bahcall, M.C. Gonzales-Garcia, and C. Peña – Garay, Phys. Rev. C **66**, 035802 (2002); JHEP **0207**, 54 (2002); New Journal of Physics, **6**, 63 (2004).
- [14] K. Eguchi et al., (The KamLAND Collaboration), Phys. Rev. Lett. **90**, 021802 (2003; Phys. Rev. Lett. **92**, 071301 (2004); T. Araki et al., Phys. Rev. Lett. **94**, 081801 (2005).

- [15] APS Multidivisional Neutrino Study, Joint Study on the future of Neutrino Physics: The Neutrino Matrix; also see C. Aalseth et al., arXiv:hep-ph/04123000.
- [16] Recommendations to the Department of Energy and the National Science Foundation on a United States Program on Neutrino-less Double Beta Decay; Submitted to the Nuclear Science Advisory Committee and the High Energy Physics Advisory Panel by the Neutrino Scientific Assessment Group, September 1, 2005.
- [17] L. Baudis et al., (The Heidelberg-Moscow Collaboration): Phys. Rev. Lett. **83**, 41 (1999); H.V. Klapdor-Kleingrothaus et al., Eur. J. Phys. A **12**, 147 (2001).
- [18] C.E. Aalseth et al., (The IGEX Collaboration): Phys. Rev. C **59**, 2108 (1999); Phys. Rev. D **65**, 092007 (2002); D **70**, 078302 (2004).
- [19] H.V. Klapdor-Kleingrothaus, A. Deitz, H.L. Harney and I.V. Krivosheina, Mod. Phys. Lett. A **16**, 2409 (2001).
- [20] H.V. Klapdor-Kleingrothaus et al., Phys. Lett. B **586**, 198 (2004); Nucl. Instrum. Methods Phys. Res., A **522**, 371 (2004); H.V. Klapdor-Kleingrothaus and I.V. Krivosheina, Mod. Phys. Lett. **21**, 1547 (2006).
- [21] C.E. Aalseth et al., Mod. Phys. Lett. A **17**, 1475 (2002).
- [22] Yu. G. Zdesenko, F.A. Danevich, and V.I. Tretyak, Phys. Lett. B **546**, 206 (2002).
- [23] Ferruccio Feruglio, Alessandro Strumia and Francesco Vissani, Nucl. Phys. B **637**, 345 (2002).
- [24] I. Abt et al., (The GERDA Collaboration) arXiv:hep-ex/0404039.
- [25] C. Arnaboldi et al., (The CUORICINO Collaboration), Phys. Lett. B **584**, 260 (2004).
- [26] C. Arnaboldi et al., (The CUORICINO Collaboration), Phys. Rev. Lett. **95**, 142501 (2005).
- [27] C. E. Aalseth et al., (The Majorana Collaboration), Nucl. Phys. B (Proc. Suppl.) **138**, 217 (2005); Also see arXiv:nucl-ex/0311013.
- [28] R. Ardito et al., (The CUORE Collaboration), arXiv:hep-ex/0501010.
- [29] M. Danilov et al., Phys. Lett. B **480**, 12 (2000); D. Akimov et al., Nucl. Phys. B (Proc. Suppl.) **138**, 224 (2005)
- [30] A.I. Belevsev et al., Phys. Lett. B **350**, 263 (1995); V.M. Lobashev et al., Phys. Lett. B **460**, 227 (1999).
- [31] Ch. Kraus et al., Eur. Phys. J. C **40**, 447 (2005).
- [32] A. Osipowicz et al., arXiv:hep-ex/0109033; V.M. Lobashev, Nucl. Phys. A **719**, 153 (2003), and references therein.
- [33] V. Barger et al., Phys. Lett. B **595**, 55 (2004).
- [34] M. Tegmark et al., Phys. Rev. D **69**, 103501 (2004).
- [35] W.J. Percival et al., astro-ph/0105252; Mon. Not. Roy. Astron. Soc., **337**, 1297 (2001); M. Colles et al., astro-ph/0106498; Mon. Not. Roy. Astron. Soc., **328**, 1039 (2001).
- [36] C.L. Bennett et al., Astrophys. J. Suppl. **148**, 1 (2003); D.N. Spergel et al., Astrophys. J. Suppl. Ser. **148**, 175 (2003).
- [37] S. Hannestad, JCAP **0305**, 004 (2003); astro-ph/0303076.
- [38] S.W. Allen, R.W. Schmidt, and S.L. Briddle, Mon. Not. R. Astron. Soc. **346**, 593 (2003).

- [39] V. Barger, D. Marfatia, and K. Whisnant, *Int. J. Mod. Phys. E* **12**, 569 (2003); see also Patric Crotty, Julien Lesgourgues, and Sergio Pastor, *Phys. Rev. D* **69**, 123007 (2004), and references therein.
- [40] M. Apollonio et al., *Phys. Lett. B* **466**, 415 (1999)
- [41] F. Boehm et al., *Phys. Rev D* **64**, 112001 (2001).
- [42] E. Fiorini and T. Niinikoski, *Nucl. Instrum. and Meth.* **224**, 83 (1984).
- [43] C. Arnaboldi, et al., *Phys. Lett. B* **557**, 167 (2003), (and references therein).
- [44] C. Arnaboldi, et al., *Nucl. Instr. And Meth. in Phys. Research A* **518**, 775 (2004).
- [45] M. Barucci, et al., *J. Low Low Temp. Phys.* **123**, 303 (2001).
- [46] G.K. White, S.J. Collocott, and J.G. Collins, *J. Phys.: Condens. Matter* **2**, 7715 (1990).
- [47] C. Arnaboldi, et al., arXiv:hep-ex/0211071; *Phys. Lett. B* **557**, 167 (2003).
- [48] A. Allessandro, et al., *Nucl. Instrum. Meth. Phys. Res. A* **142**, 163 (1998).
- [49] A. Allessandro, et al., *Nucl. Instrum. Meth. Phys. Res. A* **412**, 454 (1998).
- [50] A. Allessandro, et al., *J. Phys. D* **32**, 3099 (1999).
- [51] E.E. Haller, et al., in *Proceedings of the Fourth International Conference on Neutron Transmutation Doping of Semiconducting Materials*, National Bureau of Standards, June 1,2, 1982, Gaithersburg, MD, ed. R.B. Larrabee, Plenum Press, New York, 1984, p.21.
- [52] C. Arnaboldi et al., *IEEE Transaction Nuclear Science*, **49**, 1808 (2002).
- [53] C. Arnaboldi et al., *IEEE Transaction Nuclear Science*, **49**, 2440 (2002).
- [54] C. Arnaboldi et al., *IEEE Transaction Nuclear Science*, **50**, 979 (2003).
- [55] C. Arnaboldi et al., *IEEE Transaction Nuclear Science*, **52**, 1630 (2005).
- [56] R.M. Barnett, et al., *Phys. Rev. D* **54**,1 (1996).
- [57] S. Baker and P.D. Cousins, *Nucl. Instrum. methods. Phys. Res. A* **221**,437 (1984).
- [58] Vadim Rodin, Amand Faessler, Fedor Simkovic, and Petr Vogel, *Czech. J. Phys.* **51**, 495 (2006); arXiv:nucl-th/0602004.
- [59] V.A. Rodin, A. Faessler, F. Simkovic, and P. Vogel, *Phys. Rev. C* **68**, 044302 (2003).
- [60] V.A. Rodin, Amand Faessler, F. Simkovic, and Petr Vogel, *Nucl. Phys. A* **766**, 107 (2006).
- [61] A. Staudt, T.T.S. Kuo, and H.V. Klapdor-Kleingrothaus' *Phys. Rev. C* **46**, 871 (1992).
- [62] G. Pantis, F. Simkovic, J.D. Vergados, and A. Faessler, *Phys. Rev. C* **53**, 695 (1996).
- [63] P. Vogel, and M.R. Zirnbauer, *Phys. Rev. Lett.* **57**, 3148 (1986); *Phys. Rev. C* **37**, 731 (1988); M. Moe and P. Vogel, *Ann. Rev. Nucl. Part. Sci.* **44**, 247 (1994).
- [64]] Osvaldo Civitarese and Jouni Suhonen, *Nucl. Phys. A* **761**,313 (2005). (Their favored values were transmitted to us by private communication.)
- [65] T. Tomoda, *Rep. Prog. Phys.* **54**, 53 (1991).
- [66] C. Barbero et al., *Nucl. Phys. A* **650**, 485 (1999).
- [67] F. Simkovic, et al., *Phys. Rev. C* **60**, 055502 (1999).
- [68] J. Suhonen, O. Civitarese, and A. Faessler, *Nucl. Phys. A* **543**, 645 (1992).
- [69] K. Muto, E. Bender, and H.V. Klapdor, *Z. Phys. A* **334**, 187 (1989).
- [70] S. Stoica, and H.V. Klapdor-Kleingrothaus, *Phys. Rev. C* **63**, 064304 (2001).
- [71] A. Faessler, and F. Simkovic, *J. Phys. G* **24**, 2139 (1998).
- [72] J. Engel et al., *Phys. Lett. B* **225**, 5 (1989).
- [73] M. Aunola and J. Suhonen, *Nucl. Phys. A* **643**, 207 (1998).

- [74] R. Alvarez-Rodreguiz et al., arXiv: nucl-th/0411039; Phys. Rev. C **70**, 064309 (2004)
- [75] M. Kortelainen, O. Civitarese, J. Suhonen, and J. Toivanen, Phys. Lett. B **647**, 128 (2007).
- [76] Markus Kortelainen and Juoni Suhonen, nucl-th/0705.0469.
- [77] Erratum: of “Assessment of uncertainties in QRPA $0\nu\beta\beta$ –decay nuclear matrix elements” [Nucl. Phys. A **766**, 107 (2006): arXiv: nucl-th/0706.4304 v1.
- [78] Alfredo Poves , Talk at the ILIAS meeting, Chambéry, France, Feb. 25-28, 2007; E. Caurier, F. Nowacki and A. Poves, arXiv:0709.0277 [nucl-th].
- [80] F. Simkovic et al., arXiv: 0710.2055 [nucl-th].
- [81] Review of Particle Physics **G33**, 1 (2006), (Also see <http://pdg.lbl.gov/>).

Table 1. Central values of the numerical predictions of $\langle m_\nu \rangle$ (meV) for both hierarchies and CP phase relations. (m_1 is also given in meV.)

Normal Hierarchy				Inverted Hierarchy			
$e^{i\phi_2} = -1$		$e^{i\phi_2} = +1$		$e^{i\phi_2} = -1$		$e^{i\phi_2} = +1$	
m_1	$\langle m_\nu \rangle$	m_1	$\langle m_\nu \rangle$	m_1	$\langle m_\nu \rangle$	m_1	$\langle m_\nu \rangle$
20.0	7.90	20.0	20.2	0.00	20.0	0.00	50.0
40.0	16.0	40.0	40.0	20.0	21.6	20.0	53.9
60.0	24.0	60.0	60.0	50.0	28.3	50.0	70.7
80.0	32.0	80.0	80.0	75.0	36.0	75.0	90.1
100.0	40.0	100.0	100.0	100.0	44.7	100.0	111.0
200.0	80.0	200.0	200.0	200.0	82.5	200.	206.0
400.0	160.0	400.0	400.0	400.0	161.1	400.0	403.0

Table 2: Summary of operating parameters for the two CUORICINO data collection periods. From columns 1 through 8 are listed: the run number, number of large and small detectors, the active mass of ^{130}Te , total run time, the calibration time, the time collecting $\beta\beta$ –decay data, the total exposure in kg.y, and the usable exposure in kg.y after rejection of data not fulfilling the quality requirements. The total usable exposure is then 11.83 kg.y.

Run #	Detectors large/small	Active mass [kg ^{130}Te]	Run time [d]	Calibration [d]	t- $\beta\beta$ [d]	Collected [kg.y ^{130}Te]	Used [kg.y ^{130}Te]
1	29/15	7.95	240	24.5	55.08	1.2	1.06
2	40/15	10.37	983	108.5	415.1	11.79	10.77

Table 3. Various values of $\langle m_\nu \rangle$ corresponding to $T_{1/2}^{0\nu}(^{130}\text{Te}) = 3.0 \times 10^{24} \text{ y}$

Authors/Reference	Method	$\langle m_\nu \rangle$ (eV)
[77] Rodin <i>et al.</i> , 2007	using $2\nu\beta\beta$ -decay to fix g_{pp}	0.46
[61] Staudt <i>et al.</i> , 1992	pairing (Bohm)	0.19
[62] Pantis <i>et al.</i> , 1996	no p - n pairing	0.52
[63] Vogel, 1986		0.47
[64] Civitarese and Suhonen 2006.		0.42
[65] Tomoda, 1991		0.42
[66] Barbero, <i>et al.</i> , 1999		0.33
[67] Simkovic, 1999	pn – RQRPA	0.68
[68] Suhonen <i>et al.</i> , 1992		0.64
[69] Muto <i>et al.</i> , 1989		0.39
[70] Stoica <i>et al.</i> , 2001		0.60
[71] Faessler <i>et al.</i> , 1998		0.55
[72] Engel <i>et al.</i> , 1989	seniority	0.29
[73] Aunola <i>et al.</i> , 1998		0.41
[79] Caurier <i>et al.</i> , 2006	Nuclear Shell Model	0.58